

Retraction

Retracted: Interpolation Parameters in Inverse Distance-Weighted Interpolation Algorithm on DEM Interpolation Error

Journal of Sensors

Received 31 October 2022; Accepted 31 October 2022; Published 7 December 2022

Copyright © 2022 Journal of Sensors. This is an open access article distributed under the Creative Commons Attribution License, which permits unrestricted use, distribution, and reproduction in any medium, provided the original work is properly cited.

Journal of Sensors has retracted the article titled “Interpolation Parameters in Inverse Distance-Weighted Interpolation Algorithm on DEM Interpolation Error” [1] due to misrepresentation of images.

It was raised to our attention that the topographical images in Figure 4 have been taken from another source [2] without attribution and they do not correspond to the data presented in the article.

The authors have informed the journal that the images were intended to be representative of the data and confirmed that the images were used without obtaining the relevant permissions.

In light of this response from the authors, this article is being retracted with the agreement of the editorial board. The authors agree to the retraction.

References

- [1] Z. Liu, B. Xu, B. Cheng, and X. Hu, “Interpolation Parameters in Inverse Distance-Weighted Interpolation Algorithm on DEM Interpolation Error,” *Journal of Sensors*, vol. 2021, Article ID 3535195, 14 pages, 2021.
- [2] J. Zhang, *Research on the Adaptability of DEM Interpolation Algorithms*, PhD diss, PLA Information Engineering University, 2012.

Research Article

Interpolation Parameters in Inverse Distance-Weighted Interpolation Algorithm on DEM Interpolation Error

Zhiqiang Liu,¹ Bo Xu,¹ Bo Cheng,^{2,3} and Xiaomei Hu⁴ 

¹School of Cybersecurity, Northwestern Polytechnical University, Xi'an, 710072 Shaanxi, China

²School of Computer Science, Northwestern Polytechnical University, Xi'an, 710072 Shaanxi, China

³The Sixth Institute, 601 Branch of China Aeronautical Science and Technology Corporation, Hohhot 010076, China

⁴Shanghai Key Laboratory of Intelligent Manufacturing and Robotics, School of Mechatronic Engineering and Automation, Shanghai University, Shanghai 200072, China

Correspondence should be addressed to Xiaomei Hu; huxiaomei@oa.shu.edu.cn

Received 2 September 2021; Revised 18 November 2021; Accepted 24 November 2021; Published 24 December 2021

Academic Editor: Haibin Lv

Copyright © 2021 Zhiqiang Liu et al. This is an open access article distributed under the Creative Commons Attribution License, which permits unrestricted use, distribution, and reproduction in any medium, provided the original work is properly cited.

Although DEM occupies an important basic position in spatial analysis, so far, the quality of DEM modeling has still not reached a satisfactory accuracy. This research mainly discusses the influence of interpolation parameters in the inverse distance-weighted interpolation algorithm on the DEM interpolation error. The interpolation parameters to be studied in this paper are the number of search points, the search direction, and the smoothness factor. In order to study the optimization of IDW parameters, the parameters that have uncertain effects on DEM interpolation are found through analysis, such as the number of search points and smoothing factor. This paper designs an experiment for the optimization of the interpolation parameters of the polyhedral function and finds the optimal interpolation parameters through experimental analysis. Of course, the “optimum” here is not the only one, but refers to different terrain areas, which makes the interpolation results relatively good. The selection of search points will be one of the research focuses of this article. After determining the interpolation algorithm, the kernel function is also one of the important factors that affect the accuracy of DEM. The value of the smoothing factor in the kernel function has always been the focus of DEM interpolation research. Different terrains, different interpolations, and functions will have different optimal smoothing factors. The search direction is to ensure that the sampling points are distributed in all directions when the sampling points are sparse and to improve the contribution rate of the sampling points to the interpolation points. The selection of search shape is to improve computing efficiency and has no effect on DEM accuracy; the search radius is mainly controlled by the number of search points, and there are two methods: adaptive search radius and variable length search radius. When the weight coefficient $k = 1, 2, 3, 4$, the number of sampling points involved in the interpolation calculation is different, and the error in the residual varies greatly, and both increase with the increase of the number of sampling points in the parameter interpolation calculation. This research will help improve the quality evaluation of DEM.

1. Introduction

DEM error comes from two aspects: data error and approximation error. Most of the existing error models only take into account one aspect of the error, so they cannot truly and objectively describe the local pixel accuracy of DEM. Therefore, the DEM error is comprehensive analysis and modeling is the unavoidable tasks of DEM error model.

Interpolation method is a core issue in digital elevation model. The interpolation method always plays an important

role in the DEM production process. For example, in accuracy evaluation and accuracy analysis, interpolation algorithms often play an important role. Therefore, the research of DEM interpolation algorithm has practical significance.

Topographic analysis is the key to understanding surface processes. Herrero-Hernández et al. examined the subsurface sedimentary sequence of the Iberian Trough in Spain using geophysical techniques (simulated seismic profiles) and an inverse distance-weighted (IDW) interpolation

algorithm implemented in gvSIG open source software. They obtained digital data and quantitative isopachic maps of DS-1 and DS-2 from simulated seismic profiles. They concluded that the ancient coastline was in the direction of 150 N. Several blocks intersecting and parallel to this direction are demarcated by faults in directions between 30 N and 65 N. The thickness of sediment in these blocks varies in the nW-SE direction, with the hanging wall settling and depositing and the footwall uplifting [1]. The purpose of the Sowka study was to determine the usefulness of spatial data interpolation methods in analyzing the effects of odor on livestock facilities. The interpolation methods for the data obtained by his field olfactory measurements are the ordinary kriging (OK) method and the inverse distance weighting (IDW) method. The quality of analysis he has obtained suggests that the OK method may be better used in the presentation of spatial odor concentration distributions [2]. Zhang et al. believed that traditionally, the peak overpressure of multipoint shock wave was obtained through sensor array using electrical measurement method, and then, surface interpolation was carried out through mathematical model to draw the contour line of shock wave overpressure field. They proposed a cross-validation method of mean absolute error (MAE), mean relative error (MRE), and root mean square error (RMSE) to achieve high accuracy and effective interpolation of contour lines. They validated quantitative tests of the Kinney-Graham formula, obtaining peak multipoint shock wave overpressures for 7.62 mm guns and naval guns using polar coordinate-based sensor arrays. Then, the shock wave overpressure field was interpolated by inverse distance-weighted (IDW) interpolation, ordinary kriging interpolation (OK), radial basis function (RBF) interpolation, and cubic spline (CS) interpolation. Finally, MAE, MRE, and RMSE were analyzed by cross-validation. MAE and MRE of RBF interpolation are 0.038 and 0.001, respectively. The error is minimum, the accuracy is highest, and the interpolation effect is closest to the shock wave field model. They provided reference for isoline drawing of shock wave overpressure field [3]. Yao et al. believe that the Global Navigation Satellite System (GNSS) is now widely used for continuous ionospheric observations. 3D computer ionospheric tomography (3DCIT) is an important tool to reconstruct ionospheric electron density distribution by using GNSS data effectively. More specifically, 3DCIT enables analytical reconstruction of three-dimensional electron density distributions over a region based on GNSS tilted total electron content (STEC) observations. They proposed an improved constrained synchronous iterative reconstruction technique (ICSIRT) algorithm, which is different from traditional ionospheric tomography in three aspects [4]. Shi et al. believed that the air quality index (AQI) monitoring stations were sparsely distributed and the spatial interpolation was less accurate than the existing methods. They proposed a new algorithm based on the extended field strength model. In the single-parameter model, the strength attenuation is controlled by parameter C , while in the two-parameter model, the strength range is adjusted by additional parameter K . The optimal c and K are calculated by iterative bilinear interpolation based on the relationship between C , K , and

deviation data. They took 50 groups of AQI values monitored in Beijing, Tianjin, Wuhan, and Zhengzhou from August 2014 to April 2015 as experimental data. Based on the cross-validation and evaluation criteria RMSE, AME, and PAEE, the single-parameter model and the two-parameter model were implemented with their optimal parameters. Then, the extended field intensity model was compared with kriging and InVE using the RSE distance weighting method [5]. The Mondal et al.'s study illustrates the estimation of soil organic carbon (SOC) distribution from point survey data (prepared after laboratory test) by mixed interpolation method. In their study, they used eight selected prediction variables, such as brightness index (BI), greenness index (GI), humidity index (WI), normalized vegetation index (NDVI), vegetation temperature condition index (VTCI), digital elevation model (DEM), slope, and composite terrain index (CTI). In terms of accuracy, RK method has given satisfactory results [6]. Qin et al. report a novel nonlinear algorithm that uses support vector machines with satellite remote sensing and other types of data to retrieve near-surface temperatures over a large range. These steps include the following: (1) establish the first sub-model learning data set and validation data set and then obtain the 25th submodel learning data set and validation data set by using unmanned weather station data and predefined influence variables, (2) retrieve T_a of the target region, and (3) using inverse range-weighted interpolation to correct the T_a image generated according to the prediction error. The novelty of the algorithm lies in the application of multisource remote sensing data combined with data of unmanned weather stations, topography, land cover, DEM, astronomy, and calendar rules [7].

This research mainly discusses the influence of interpolation parameters in the inverse distance-weighted interpolation algorithm on the DEM interpolation error. The interpolation parameters to be studied in this paper are the number of search points, the search direction, and the smoothness factor. In order to study the optimization of IDW parameters, the parameters that have uncertain effects on DEM interpolation are found through analysis, such as the number of search points and smoothing factor. After determining the interpolation algorithm, the kernel function is also one of the important factors that affect the accuracy of DEM. The value of the smoothing factor in the kernel function has always been the focus of DEM interpolation research. Different terrains, different interpolations, and functions will have different optimal smoothing factors.

2. Methods

2.1. Essence and Characteristics of DEM Generation. As one of the basic data of national geographic information, DEM contains a variety of important information such as terrain surface morphology. Both users and producers hope that the higher the accuracy of DEM, the better. For a long time, the reasonable selection of interpolation function is one of the methods to improve the accuracy of DEM. The interpolation essence of the commonly used interpolation methods is the same; that is, the elevation value of the point to be

inserted is obtained by interpolation according to the elevation value of the known ground point data. The ground is a very complex irregular surface, but it is regarded as a set of infinite points, but it is impossible to get infinite ground points in the actual data acquisition process; only limited discrete data points can be obtained. Therefore, the mathematical method should be used to change infinity into finiteness. The elevation of the unknown point can be obtained through the interpolation of the known discrete point data, and the mathematical model can be established. The elevation value of any point can be obtained through the established model.

Whether it is an ordinary map, a contour map, or an image, it is a simulation and expression of the three-dimensional real world in a two-dimensional environment. For the expression of topographic surface morphology, on the one hand, it is necessary not only to consider the issue of scalability but also to consider the visual and physiological feelings, which means that the scalability of two-dimensional expression and the expression of three-dimensional model are inherently impossible. Coexisting, there is an insurmountable gap between the expression of two-dimensional space and the three-dimensional real world represented. As a way of expressing important information such as important surface morphology, DEM also has its own characteristics: (1) Surface morphology information can be presented in various forms. (2) Compared with traditional paper topographic maps, the accuracy is not easy to lose. (3) It is easier to achieve graphic processing and expression automation of and the real-time update of map information. (4) It has multiscale characteristics. It is precisely because of these characteristics of DEM that DEM has been widely used in all walks of life in social production activities. The basic principle of DEM is shown in Figure 1.

Digital elevation model, as the basic data for the development of various industries, especially the local information industry, has produced huge demands in both application and research. Generally, we divide the representation method of DEM into three categories, namely, contour method, irregular grid method, and regular grid method.

The relationship between the difference in accuracy of data with and without additional feature points and grid spacing is as follows [8]:

$$\Delta\sigma = \sigma_r - \sigma_e = A + B \times d^2, \quad (1)$$

where d represents the grid spacing and A and B are the constants. The data accuracy of the bilinear interpolation of the grid is divided into isosceles right angle TIN [9]:

$$\sigma^2 = \frac{1}{3}\sigma_p^2 + \frac{7}{12}(K \times Dx \tan \beta)^2. \quad (2)$$

K is a constant smaller than Dx . Use the difference between the elevation of a point in the grid and the average of the elevations of the four vertices of the grid to describe the terrain descriptive error [10]:

$$E = H - H_O = \frac{H_O - (H_A + H_B + H_C + H_D)}{4}. \quad (3)$$

Suppose the area of the Thiessen polygon P to be inserted is a , then [11]:

$$Z_p = \sum_{i=1}^n \frac{a_i}{a} z_p. \quad (4)$$

The triangulated irregular network is a sampling representation system specially designed for generating DEM data. The TIN model connects these discrete points (the vertices of each triangle) into mutually continuous triangles according to the discrete data obtained by all sampling points in the area, and according to the principle of optimal combination, make each triangle as an acute triangle or as possible when connecting. The lengths of the three sides are approximately equal. The expression of the plane equation is follows [12]:

$$z = ax + by + c. \quad (5)$$

The solving equation of coefficients a , b , and c is follows [13]:

$$\begin{bmatrix} a \\ b \\ c \end{bmatrix} = \begin{bmatrix} x_A & y_A & 1 \\ x_C & y_B & 1 \\ x_C & y_B & 1 \end{bmatrix}. \quad (6)$$

So, the estimated value of Z_p is as follows [14]:

$$Z_p = \begin{bmatrix} x_p & y_p & 1 \end{bmatrix} \begin{bmatrix} x_A & y_A & 1 \\ x_B & y_B & 1 \\ x_C & y_C & 1 \end{bmatrix}^{-1} \begin{bmatrix} z_A \\ z_B \\ z_C \end{bmatrix}, \quad (7)$$

$$A = \begin{bmatrix} x_p & y_p & 1 \end{bmatrix}.$$

The function expression of the quadratic polynomial is as follows [15]:

$$z_p = \beta_0 + \beta_1 x + \beta_2 y + \beta_3 x^2 + \beta_4 y^2 + \beta_5 xy. \quad (8)$$

Then, based on the principle of least squares, it is not difficult to obtain the coefficient vector [16]:

$$B = [P^T P]^{-1} P^T Z. \quad (9)$$

So, the height of the point to be inserted is as follows [17]:

$$z_p = AB = A [P^T P]^{-1} P^T Z. \quad (10)$$

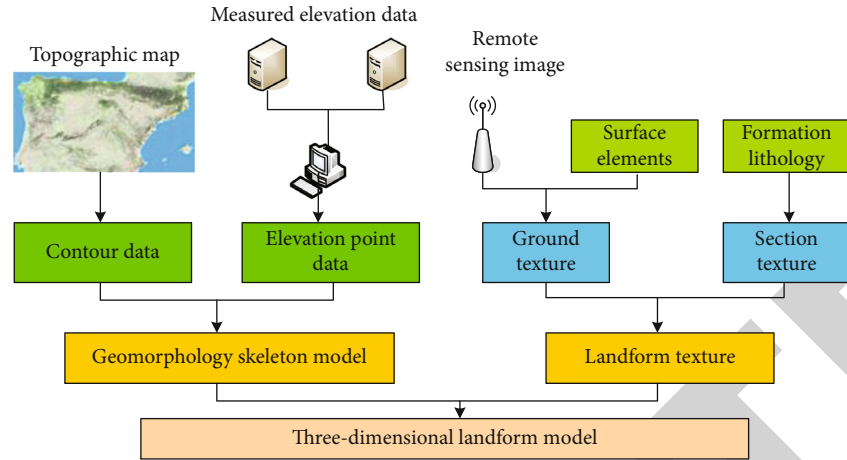


FIGURE 1: Basic principle of DEM.

It is to introduce a basis function $g(x)$ for each known point P :

$$f(x) = \sum_{i=1}^n g(x_i)y. \quad (11)$$

The basis function can be constructed like this [18]:

$$g(x) = \frac{(x - x_1)(x - x_2) \cdots (x - x_n)}{(x_1 - x_2)(x_2 - x_3)(x_3 - x_4) \cdots (x_i - x_n)}. \quad (12)$$

2.2. Main Sources of DEM Data. Topographic map is a main data source of DEM. As we all know, almost all countries in the world have their own topographic maps. In many developing countries, topographic maps do not cover all their territories. In most developed countries, the topographic map with high-quality contour information basically covers all land, which provides a rich and cheap data source for DEM construction. The same is true of some developing countries, such as China. However, there are also the following deficiencies:

- (1) The reality of topographic maps is poor: (1) the production process of paper topographic maps is relatively complicated, which makes its update relatively slow. For the rapidly changing high-tech development zones, the paper topographic maps cannot reflect the real elevation information in time; for sparsely populated, basic unchanging topography and landforms with slow development of modernization, the existing topographic maps will be the data source of high quality and low price
- (2) Due to environmental factors such as temperature and humidity, the topographic map produces various deformations. The accuracy of the existing topographic maps may not necessarily meet the actual needs
- (3) Photogrammetry and remote sensing image data collect (measure) electromagnetic wave information radiated or reflected by ground objects through sen-

sors installed on the platform and convert them into images, and then according to the spectral characteristics of various ground objects that have been mastered, analyze and process this information to get the required information. For example, synthetic aperture radar interferometry, airborne laser scanning, vehicle-mounted mobile laser scanning, and aerial photogrammetry are all effective methods for DEM data acquisition

- (4) The DEM structure scale includes the horizontal direction scale and the vertical direction scale. The horizontal direction scale is the horizontal resolution, also known as the horizontal sampling interval, grid unit, grid spacing, etc., which is commonly referred to as DEM resolution, which is the most basic of DEM. One of the variables of its size directly determines the accuracy of DEM's description of the ground. The vertical dimension is the vertical resolution of the DEM. There are many methods to collect DEM data directly from the ground, such as global positioning system (GPS). However, this data acquisition method has a large workload, long cycle, low efficiency, difficult updating, and high cost, so it cannot be used when the acquisition area is large. The DEM data processing method in this study is shown in Figure 2

2.3. Inverse Distance-Weighted Interpolation. The basic principle of inverse distance-weighted (IDW) interpolation method is the similar principle: each interpolation point has an influence on the interpolation point, and its influence is called weight. The weight is assigned by the distance between the point to be interpolated and the interpolation point, that is, the smaller the distance, the greater the weight, and vice versa, the smaller the weight. At the same time, when the distance between the two is outside a certain range, the contribution of the interpolation point to the elevation of the interpolation point can be ignored; that is, the weight is zero. The formula of the inverse distance-weighted interpolation method is as follows [19]:

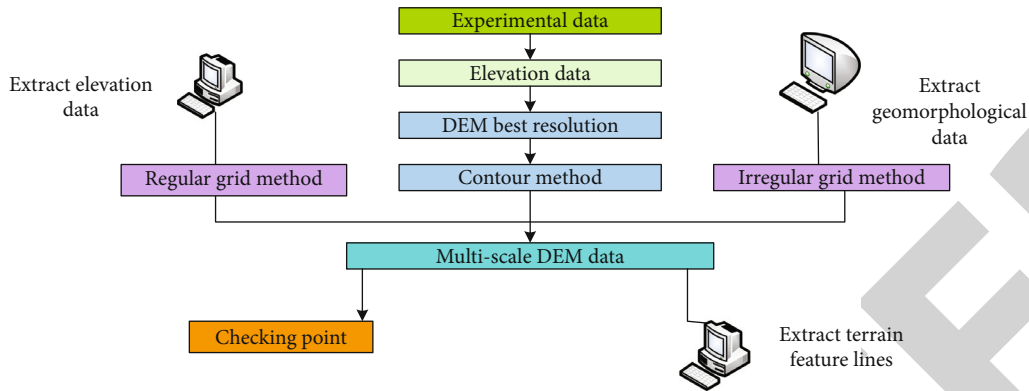


FIGURE 2: DEM data processing method in this study.

$$Z(p) = \sum_{i=1}^n \beta Z(s), \quad (13)$$

where $Z(p)$ is the elevation value of the point to be interpolated; n is the number of interpolation points used when calculating the elevation of the point to be interpolated; β is the weight of the corresponding interpolation point; $Z(s)$ is the elevation value of each interpolation point. The calculation formula for determining the weight is as follows [20]:

$$\beta_i = \frac{d_i^{-u}}{\sum_{i=1}^n d_i^{-u}}, \quad (14)$$

$$\sum_{i=1}^n \beta_i = 1.$$

Among them, u has the effect of reducing the influence of other locations as the distance increases. When $u = 0$, the distance does not affect the specific choice of the power index which depends on the specific conditions of the study area. The influencing factors of inverse distance-weighted interpolation are shown in Figure 3.

The weight coefficient in the inverse distance-weighted interpolation is d_i^{-u} , which is an important factor that affects the accuracy of the interpolation, and it assigns the size of the sampling point to participate in the interpolation. The weight coefficient for d_i^{-u} is a decay function. It can be seen from Figure 3 that as the distance between the sampling point and the interpolation point increases, the weight coefficient decreases, indicating that the correlation between the two points also decreases as the distance increases.

When performing inverse distance-weighted interpolation of terrain data, when k is the best value, the interpolation effect can be determined by cross-validation method. Know the sampling point, obtain its elevation value through inverse distance-weighted interpolation, and compare the measured elevation value with the elevation prediction value [21]:

$$Q = \frac{\sum_{i=1}^n (Z(p) - Z^*(p))^2}{n}. \quad (15)$$

The smaller the Q value, the more reasonable the value of u . Whether the number of sampling points m involved in the interpolation calculation will also affect the interpolation accuracy is also determined by the cross-validation method. Assuming N sampling points, $Z(p)$ and $Z^*(p)$ are the actual values and inverse distance-weighted interpolation prediction values of N sampling points, respectively, and the residuals are as follows [22]:

$$\Delta_i = Z(p) - Z^*(p). \quad (16)$$

Residual mean the following:

$$p = \frac{\sum_{i=1}^N \Delta_i}{N}. \quad (17)$$

Error in residual is as follows:

$$\sigma = \sqrt{\frac{|\Delta - p|}{N - 1}}. \quad (18)$$

2.4. IDW Parameter Optimization Experiment. DEM is a digital terrain model. The digital elevation model expresses the continuously changing terrain surface in a discrete manner, which is bound to be constrained by various scales. Different scales of DEM have significant differences in the degree of refinement of terrain expression, and the research objects of different geographic scales DEM of the corresponding scale should be selected with the content. DEM and terrain analysis have obvious scale dependence.

In order to study the optimization of IDW parameters, the parameters that have uncertain effects on DEM interpolation are found through analysis, such as the number of search points and smoothing factor. This paper designs an experiment for the optimization of the interpolation parameters of the polyhedral function and finds the optimal interpolation parameters through experimental analysis. Of course, the “optimum” here is not the only one, but refers to different terrain areas, which makes the interpolation results relatively good. A fuzzy value of a parameter, or a range of values, can provide a reference for the user to select appropriate interpolation parameters for different terrains

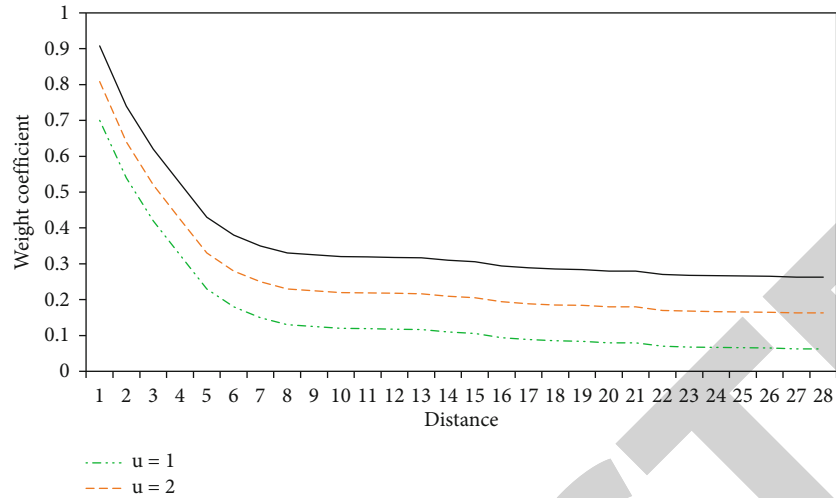


FIGURE 3: Influencing factors of inverse distance-weighted interpolation.



FIGURE 4: Landforms of different test areas.

and interpolation kernel functions in the process of multifaceted function interpolation. The topography of different test areas is shown in Figure 4.

Scale up is that geographic information obtains coarse spatial resolution from fine spatial resolution. Its essence is the generalization and synthesis of information, the reduction of resolution and the increase of breadth, and the reduction of spatial heterogeneity. Scale down is that geographic information obtains fine spatial resolution from coarse spatial resolution. Its essence is to express spatial targets more finely and microscopically. As spatial information increases, spatial heterogeneity increases, which is the redistribution of information. According to our country's topographic undulations, it is divided into plains (undulations < 30 m), mesa (undulations > 30 m), hills (undulations < 200 m), low mountains (undulations of 200-500 m), middle mountain (undulations of 500-1000 m), high mountain (undulation degree is 1000-2500 m), and extremely high mountain (undulation degree > 2500 m). The data of these five regions are selected based on this, and the results of the division are shown in Table 1.

2.5. Uncertainty of Interpolation Parameters. After determining the interpolation algorithm, the main factor that affects DEM accuracy is the interpolation parameters. In the search mode, both the search shape and the search radius are determined to meet the requirements of the number of search points. The selection of search shape is to improve computing efficiency and has no effect on DEM

accuracy; the search radius is mainly controlled by the number of search points, and there are two methods of adaptive search radius and variable length search radius; these two parameters are determined; right DEM interpolation accuracy has no big impact. Considering the influence of contour lines, fracture lines, boundary lines, and other characteristic lines in the interpolation process will inevitably improve the DEM accuracy. This is no doubt, but it is more complicated to consider the influence of characteristic lines in the interpolation algorithm. The search direction is to ensure that the sampling points are distributed in all directions when the sampling points are sparse and to improve the contribution rate of the sampling points to the interpolation points. The selection of search points will be one of the research focuses of this article. After determining the interpolation algorithm, the kernel function is also one of the important factors that affect the accuracy of DEM. The value of the smoothing factor in the kernel function has always been the focus of DEM interpolation research. Different terrains, different interpolations, and functions will have different optimal smoothing factors. In summary, the interpolation parameters to be studied in this paper are the number of search points, search direction, and smoothness factor.

3. Results

Digital elevation model data is the most important source of spatial information in the geographic information system database and is the core database for three-dimensional

TABLE 1: Results of regional division.

Landform type	Plain	Hills	Low mountain	Middle mountain	Alpine
Area	Jiangsu	Shandong	Henan	Guizhou	Sichuan
Minimum elevation/m	2	147	392	1047	3151
Highest elevation/m	27	294	783	1776	4527
Average slope/(°)	1.5	8.6	14.7	21.6	33.9

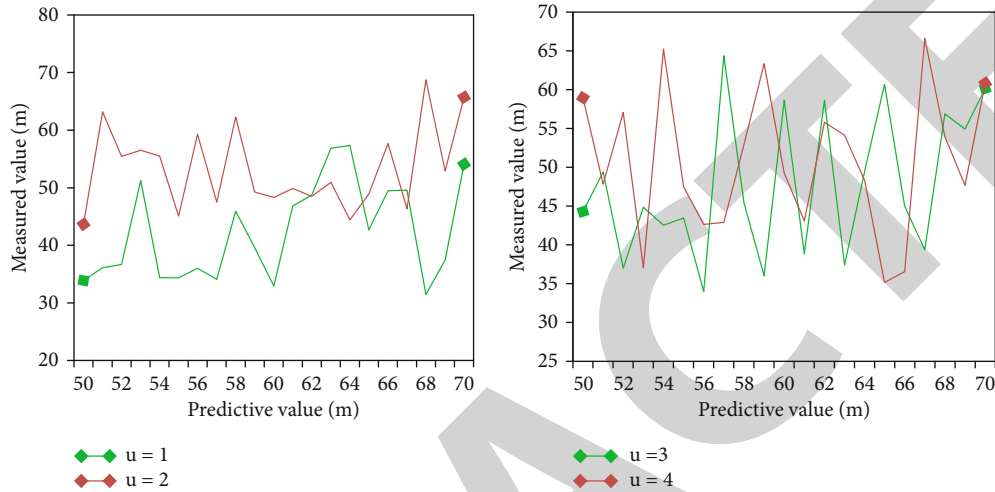


FIGURE 5: Scattered relationship between measured values and predicted values of sampling points.

spatial processing and terrain analysis. A variety of topographic factors can be derived from it, such as microtopographic factors: slope, aspect, slope length, slope variability, aspect variability, plane curvature, profile curvature, etc.

This experiment uses the 16 sampling points closest to the known sampling points as the interpolation calculation points to perform cross-validation to obtain the Q values under $k = 1, 2, 3, 4$, where $Q_1 = 0.1624$, $Q_2 = 0.2576$, $Q_3 = 0.1036$, and $Q_4 = 0.4366$. The comparison of Q values shows that when $u = 3$ in the weight coefficient, the inverse distance-weighted interpolation algorithm has the best interpolation effect. When u takes different values, the scatter relationship between the actual measured value and the predicted value of the sampling point is shown in Figure 5. It shows that when the number of points involved in the interpolation calculation is certain, the value of u in different weight coefficients affects the accuracy of the interpolation, so the inverse distance-weighted interpolation needs to choose a suitable value of u .

Assuming that the weight coefficient $u = 3$ in the inverse distance-weighted interpolation parameter, the number of sampling points m participating in the interpolation calculation is 4, 10, 16, 22, 28, 34, 40, 46, 52, and 58, respectively, and cross-validation calculation is performed. Take the error in the residual to compare and determine the influence of the number of sampling points m participating in the interpolation calculation on the interpolation effect. Cross-validation is performed to obtain the residual errors in different situations. The calculation results are shown in Table 2. It can be seen from Table 2 that when the number of sampling points involved in the calculation is 10 and 16,

the error in the residual is close to the smallest. It shows that the number of sampling points involved in the interpolation calculation should take an appropriate value, more or less, will have an adverse effect on the interpolation effect and reduce the interpolation accuracy.

When studying the influence of the number of points involved in the interpolation calculation on the accuracy of the inverse distance-weighted interpolation, the value of u in the weight coefficient is kept unchanged. When studying the interactive effects of the two parameters in this study, when $u = 1, 2, 3, 4$, the number of sampling points m participating in the interpolation is taken as 4, 10, 16, 22, 28, and 34 for cross-validation. The errors in the residuals are compared in various situations, and the comparison results are shown in Figure 6. Because the difference between the errors in the calculated residuals is very small, when drawing, the error values in the residuals are uniformly multiplied by 10.

When the weight coefficient $k = 1, 2, 3, 4$, the number of sampling points involved in the interpolation calculation is different, and the error in the residual varies greatly, and both increase with the increase of the number of sampling points in the parameter interpolation calculation. When the number of sampling points involved in the interpolation calculation is fixed, when the value of k in the weight coefficient is different, the error in the residual is different, and when $k = 3$, the error in the residual reaches the minimum. Experiments show that when inverse distance-weighted interpolation is performed on the point cloud data in this study, the interpolation accuracy is affected by both the k value in the weight coefficient and the number of sampling points participating in the interpolation calculation m . The

TABLE 2: Do not find the residual error in different situations.

Participated in the calculation of points	4	10	16	22	28
Error in residual σ (m)	0.3510	0.3216	0.3220	0.3258	0.3271
Participated in the calculation of points	34	40	46	52	58
Error in residual σ (m)	0.3291	0.3303	0.3339	0.3359	0.3372

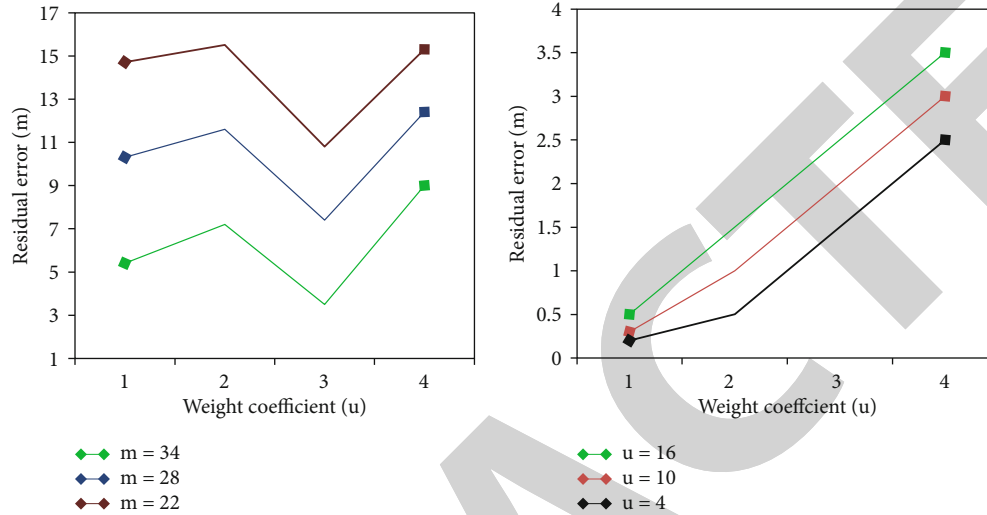


FIGURE 6: Comparison of residual errors in various situations.

k value in the weight coefficient has a greater impact on the interpolation accuracy than the interpolation calculation. The number of sampling points m is determined by the cross-validation method to determine the optimal parameters for the inverse distance-weighted interpolation of the point cloud data in this paper: the number of sampling points involved in the interpolation calculation is 10-16, and the weight coefficient k is 3.

This article introduces the three interpolation methods of kriging, inverse distance weighting, and nearest neighbor points to spatially interpolate the attribute values of the grid points in the area where the point cloud data is located and compare the obtained results with the original point cloud data. Due to the amount of point cloud data huge, this study only extracted a small part of the point cloud data interpolation results shown in Table 3.

The maximum residual error in the inverse distance-weighted interpolation result is 1.89 m, the maximum residual error in the kriging interpolation result is 4.9 m, and the maximum residual error in the nearest neighbor interpolation result is 6.99 m. According to statistical data, we draw its residual histogram as shown in Figure 7. From the distribution of the residual distribution histogram, the residual distribution in the inverse distance-weighted interpolation result is better than the kriging interpolation and nearest neighbor interpolation residual distribution.

The smaller the values of the three evaluation indexes MAE, MRE, and RMSE are, the higher the interpolation accuracy is. Calculate the average absolute error, average relative error, and median error between the predicted elevation value under various interpolation methods and the

actual elevation value of the original point cloud data. The statistical results are shown in Table 4.

Among the three methods of kriging interpolation, inverse distance-weighted interpolation, and nearest neighbor interpolation, the three evaluation indicators of the kriging interpolation method are less than the other two methods, indicating that the inverse distance-weighted interpolation has the highest accuracy, and the kriging interpolation is the second. The nearest neighbor interpolation has the lowest accuracy.

Use the inverse distance-weighted interpolation algorithm to interpolate the experimental point cloud data, compare the interpolation results with the original point cloud data, and use the relevant evaluation indicators to evaluate the accuracy of the interpolation results. The results are shown in Table 5.

To study the effect of the number of search points on DEM accuracy, first determine the search direction as nondirection search (that is, the search direction is not tested, and the total number of search points meets the requirements), and the smoothing factor is determined (the values are 0, 60, 100, 600, and 1000) to conduct experiments in different experimental areas. Taking the number of search points h as the horizontal axis and the error in the global residual as the vertical axis, each curve represents the influence of the number of search points on the DEM interpolation accuracy when the smoothness factor is different.

In the plain experimental area, as the number of search points increases, when the smoothing factor is 0, the median error first decreases rapidly (the number of search points is

TABLE 3: Interpolation results of a small number of point cloud data.

ID	Coordinate value		Raw point cloud data	Inverse distance-weighted data	Kriging interpolation data	Nearest neighbor data
	X (m)	Y (m)	Z (m)	Z (m)	Z (m)	Z (m)
1	179.5	94.5	66.3289	66.6764	67.8528	66.8078
2	179.5	95.5	68.2345	67.3349	67.5963	68.5148
4	179.5	96.0	67.9607	67.9414	67.758	68.5148
5	179.5	96.5	67.6036	67.8058	68.0744	67.4243
6	179.5	97.0	67.4243	67.4243	67.7572	67.4243

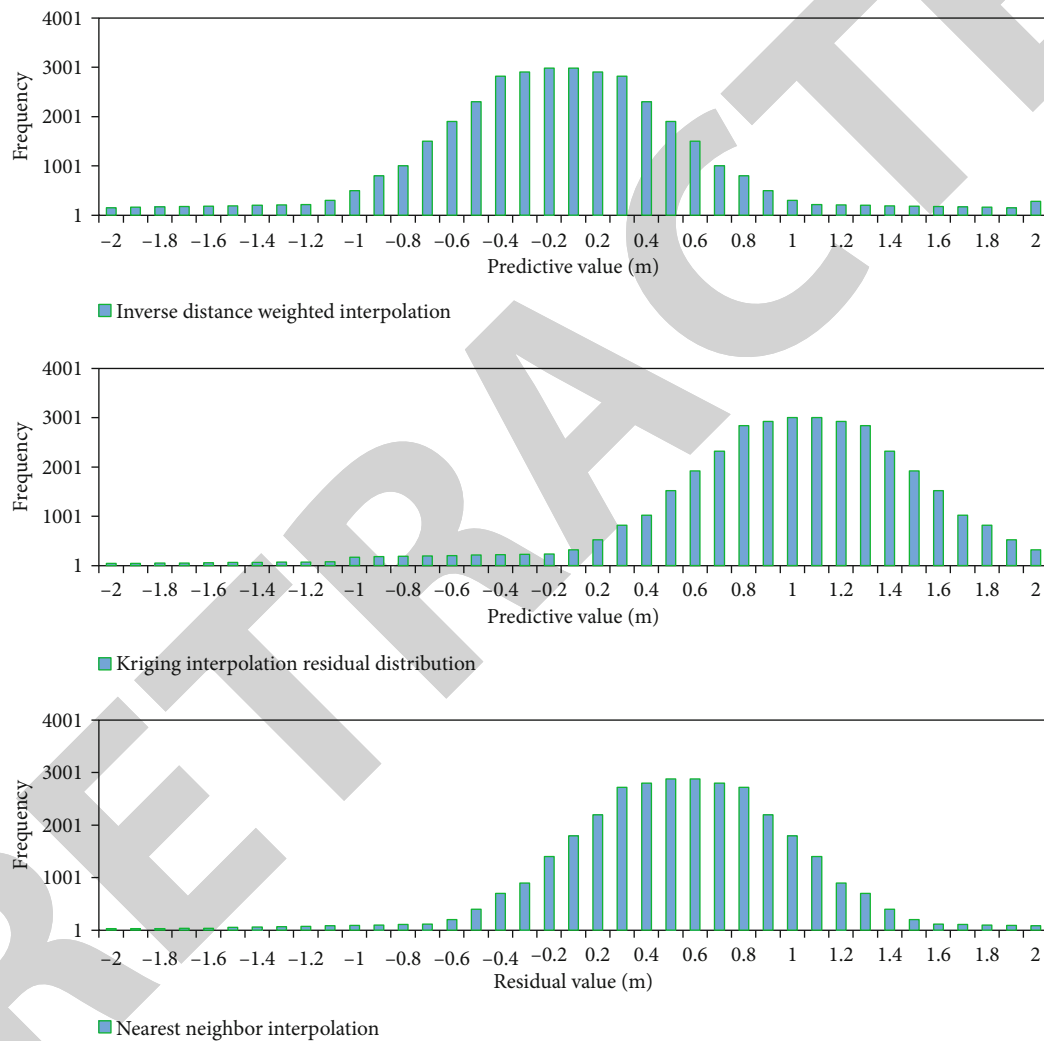


FIGURE 7: Histogram of residuals.

4-10), then slowly decreases (the number of search points is 10-30), and then basically remains stable. When the smoothing factor is selected other four values, the overall trend of the error is the same; that is, it decreases first, and it basically reaches the minimum when the number of search points is 10, and then increases at a different speed. It can be seen that if the influence of the smooth factor is not considered, the number of search points is 10 which is the most appropriate, but this is not the number of search points corresponding to

the minimum error; when the number of search points is 30 or greater, there is a corresponding smooth factor that can make the middle error smaller. The results of the search points in the plain experimental area are shown in Figure 8.

As the basic data of national geographic information, digital elevation model (DEM) is the framework data of National Spatial Data Infrastructure (NSDI), which has important applications in the national economy and national defense construction. With the coexistence of

TABLE 4: Comparison of average absolute error, average relative error, and median error.

Interpolation method	Mean absolute error (m)	Average relative error	Medium error (m)
Inverse distance-weighted interpolation	0.0840	0.0012	0.15
Kriging interpolation	0.2453	0.0034	0.41
Nearest neighbor interpolation	0.2705	0.0038	0.52

TABLE 5: Comparison of interpolation results and original point cloud data.

Analysis scope	Mean absolute error (m)	Average relative error	Medium error (m)
Void area	0.900	0.0128	1.2588
Area outside the cavity	0.063	0.0009	0.1217
All areas	0.085	0.0012	0.2408

DEMs with different scales, different resolutions, and different precisions, the issue of DEM scale is a hot issue that needs to be solved urgently [23, 24].

In the hilly experimental area, as the number of search points increases, the change trend of the median error is also different due to the different values of the smoothing factor. There are basically two situations: first decrease, and then remain stable after reaching a certain value; second, decrease first, and the middle error will increase in turn after reaching a certain value. When the smoothing factor is 0, there is no turning point, and finally, it remains stable. When the smoothing factor takes other values, the turning point is 10 search points. Similar to the plain experimental area, the optimal number of search points is 10 without considering the smoothness factor. But when the number of search points is 30 or more, there will be a suitable smoothing factor to make the median error smaller. The results of the search points in the hilly experimental area are shown in Figure 9.

DEM is an expression of the surface morphology and should reflect the amount of terrain information to the greatest extent. This needs to start with the original data and explore the method of determining DEM resolution. Using fractal to quantitatively express the characteristics of terrain self-similarity and complexity, the relationship between DEM resolution and fractal information dimension is established, and the inflection point that can describe the terrain information to the maximum is sought through the slope difference of the straight line, so as to determine the horizontal resolution of DEM [25].

In the low mountain experimental area, similar results were obtained in the plain and hilly experimental area. The number of search points of about 30 is obviously better than that of 10 search points (when a reasonable smoothing factor is obtained). In other words, when there are 30 search points, there is a smaller median error than when there are 10 search points. Similarly, take the search points as 15, 20, 30, 40, and 50 to make a graph. With the increase of the smoothing factor, the median error increases first, decreases after reaching a certain value, and then increases rapidly. There are two intervals with better smoothness factors: one is near 0 and the other is between 200 and 400. You can

observe the changes in errors more clearly. Obviously, when $c = 0$, no matter what the number of search points is, a small median error is obtained, especially when the number of search points is 40-50. In addition, when the number of search points is about 50 and the smoothing factor is about 250, the median error value is the smallest. The DEM analysis result of the low mountain experimental area is shown in Figure 10.

4. Discussion

The DEM scaling algorithm based on multiband wavelet decomposition is studied. Starting from the actual application requirements of DEM, the basic principle of DEM scale up is established. Taking into account the accuracy factors of DEM scale upscaling, a DEM scale upscaling algorithm based on random numbers is constructed. Using the characteristics of multiresolution analysis and multiscale analysis of multifrequency wave, a method of DEM scale-up reduction based on multiband wavelet decomposition is proposed [26]. In essence, a map is a scientific generalization (synthesis) and abstraction of the objectively existing features and changing rules. For the most typical and important topographic map in the map, because the objective world describes is a colorful and varied three-dimensional space entity, there is an insurmountable relationship between the expression of its two-dimensional space and the three-dimensional real world it represents. Because of this, cartographic scholars have been devoted to the three-dimensional representation of topographic maps for thousands of years, trying to find a representation method that can not only conform to people's visual and physiological habits but also restore the real topographical world. DEM is a mathematical model of the terrain surface. Mathematically speaking, the elevation model is a two-dimensional continuous function. Therefore, DEM is the discrete representation of the elevation model. The representation methods of DEM can be divided into three categories, namely, regular grid model, contour model, and irregular triangulation method. Among them, regular grid model is the most commonly used model. In data collection, many of the original data obtained are in the form of discrete points. In practical applications, it is necessary to use the DEM interpolation algorithm to generate a regular grid model. Using spatial interpolation algorithm to interpolate terrain can effectively analyze geological body information. With the continuous development of computer visualization technology in recent years, the expression of ore bodies is realized through three-dimensional modeling. Some discrete sample points with known grade and other information can

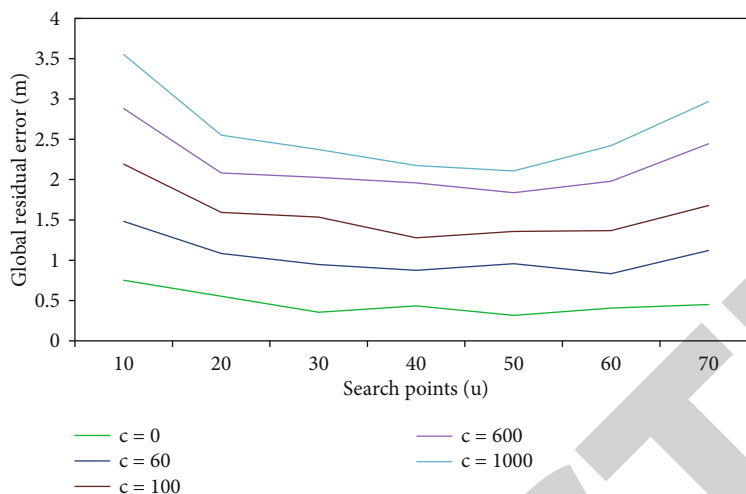


FIGURE 8: Results of search points in the plain experimental area.

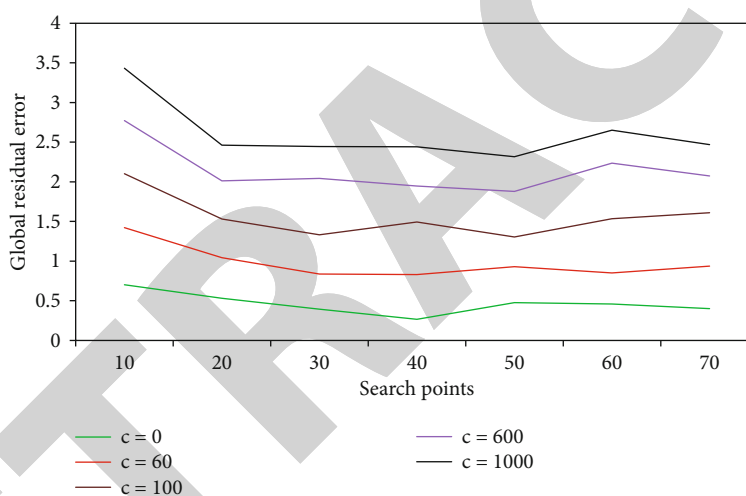


FIGURE 9: Results of search points in the hilly experimental area.

be used to perform sample points with unknown information within a certain range [27, 28].

Before using the DEM error model, the terrain data should be preprocessed to make it conform to the assumption of a stable random process, so as to improve the reliability of DEM accuracy estimation. The surface usually has a specific overall trend, such as the slope of the terrain, the trend of the slope, the depression of the basin, and the uplift of the mountains and hills; the trend is a certain amount of definite analytical formula, which can be determined by the trend surface analysis. After removing the trend, what remains is the random residual, including the correlated random part and the uncorrelated random part (white noise). The correlated random part has a specific spatial autocorrelation (the closer the distance, the more similar the value). For terrain data, the residual amount after removing the trend can be considered as a stationary random process, and the covariance function of the random process can be estimated through statistical analysis.

The covariance function is a function of distance, usually a monotonically decreasing positive even function. When the local table changes more complexly, its trend surface is relatively more complicated. When selecting the trend surface equation, a preliminary analysis of the terrain data should be carried out, and a visualization method should be used, that is, by comparing the covariance cloud diagrams of various trend surfaces, the more convergent the covariance cloud diagram, better the fit with the empirical covariance function, the better the stability of the terrain data, and the higher the reliability in the DEM accuracy prediction [29].

Obtaining the accuracy of DEM pixels is the basic goal of DEM error model research, and its ultimate goal is the application of error model, that is, how to provide theoretical support for the reliability evaluation of DEM data modeling strategy and DEM engineering application and analysis. First, the DEM error model can in turn guide DEM data sampling. DEM terrain data sampling is one of the main

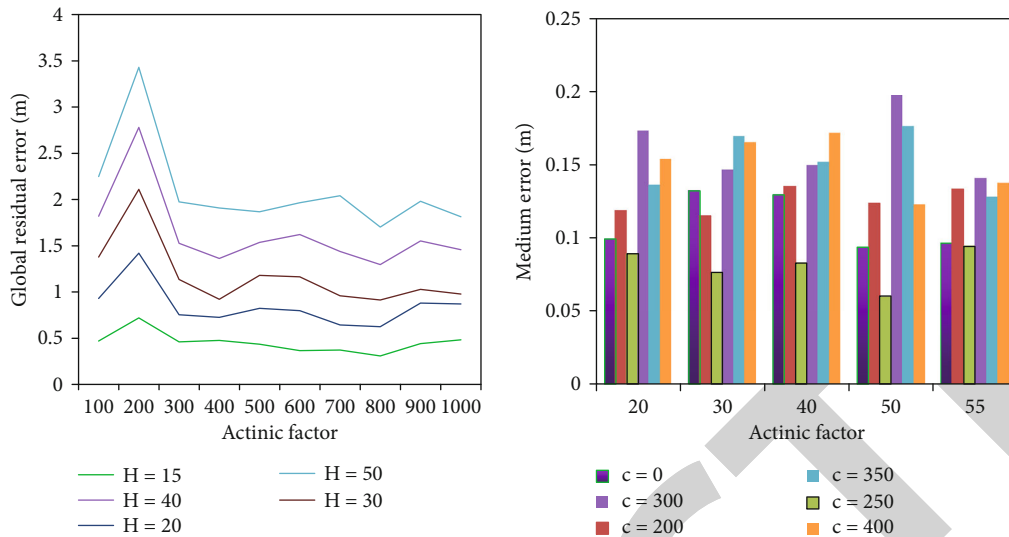


FIGURE 10: DEM analysis results of low mountain experimental area.

factors that cause DEM errors. DEM data sampling should take into account the characteristics of the terrain itself. Of the same amount of data collection, a good terrain data sampling strategy can significantly reduce DEM errors. Like traditional topographic field surveying, the basic principle of digital elevation model data sampling points is to restore and reconstruct the terrain surface through the fewest sampling points. Whether it is random distribution sampling, regular distribution sampling, progressive sampling, selective sampling, or mixed sampling, although it is designed for terrain elevation sampling based on the above principles, it has universal significance; that is, they are also suitable for collection of nonelevation data in geographic information systems such as geology, soil, climate, and other data [30, 31].

A DEM scaling algorithm based on the combination of multiband wavelet and interpolation is proposed. First, use multiband wavelet decomposition to perform bilinear interpolation of the obtained high-frequency part and use it as the low-frequency part with the original DEM data. Through multiband wavelet inverse transformation, the scale-down DEM data is obtained, and the experimental results of subjective and objective evaluations were made. Second, the study of DEM error model will provide decision support and evaluation criteria for DEM application and analysis. In the evaluation of DEM data applicability, DEM error model can solve the accuracy evaluation problems of various applications, so the model accuracy can provide decision support for users in the evaluation of DEM applicability: in the evaluation of DEM interpolation model, DEM error model generates DEM accuracy fields of various interpolation models, and finally, the advantages and disadvantages of DEM interpolation model can be found according to comparison and statistics. In the evaluation of inverse distance-weighted interpolation algorithm, because DEM error model can generate accuracy field, it can evaluate the advantages and disadvantages of IDW algorithms more scientifically and objectively [32].

5. Conclusion

People live on the earth and are in contact with the earth's surface everywhere. Although people from all walks of life have different needs and research focuses, they have a common hope: to express actual surface phenomena in a convenient and accurate way. In the early stage, surveying knowledge and technology were relatively scarce, and people could not truly reproduce the surface shape and mainly used pictograms to depict the terrain. Based on the in-depth and systematic study of DEM model establishment and contour formation, this paper uses different terrain feature data to conduct experiments. Resample the contour map, generate DEM data, and establish contour lines. A new method for judging the quality of contour lines is adopted. The data fusion of DEM has been analyzed theoretically and experimentally to test the influence of data fusion on the final quality of DEM. Based on the inverse distance-weighted interpolation algorithm, efforts have been made to improve the quality of DEM. As the foundation of geospace science, DEM has huge development prospects. At the same time, DEM is also playing an important role; for example, it plays an important role in analyzing terrain data in geographic information system (GIS) database. The DEM error model can theoretically complete the modeling and expression of the local accuracy of the DEM and analyze the spatial structure of the DEM error. However, due to the multisource nature of the DEM data source and the wide range of DEM applications, the DEM accuracy research work faces new research content.

Data Availability

No data were used to support this study.

Conflicts of Interest

There is no potential conflict of interest in this study.

References

- [1] A. Herrero-Hernández, F. J. López-Moro, M. E. Valle-Feijóo, F. Gómez-Fernández, and J. R. Rodríguez-Pérez, "Mapping of tecto-lineaments and their influence on sedimentological processes in a GIS environment: a case study of the Iberian trough, Spain," *Geologica Carpathica*, vol. 68, no. 2, pp. 165–174, 2017.
- [2] I. Sówka, A. Grzelka, M. Pawnuik, and A. Pielichowska, "The use of ordinary kriging and inverse distance weighted interpolation to assess the odour impact of a poultry farming," *Scientific Review Engineering and Environmental Sciences*, vol. 29, no. 1, pp. 17–26, 2020.
- [3] Y. Zhang, T. Han, L. Hong, X. Wang, and E. Zhang, "Cooperation of the spatial interpolation algorithm for the contour map of the shockwave overpressure field," *Journal of Engineering Science and Technology Review*, vol. 10, no. 6, pp. 104–110, 2017.
- [4] Y. Yao, C. Zhai, J. Kong, C. Zhao, Y. Luo, and L. Liu, "An improved constrained simultaneous iterative reconstruction technique for ionospheric tomography," *GPS Solutions*, vol. 24, no. 3, pp. 1–19, 2020.
- [5] Z. Shi, J. Zhao, W. Zhang, Y. Hu, and X. Wu, "New spatial interpolation algorithm for sparse AQI based on extended field intensity model," *Geomatics & Information Science of Wuhan University*, vol. 42, no. 7, pp. 968–974, 2017.
- [6] A. Mondal, D. Khare, S. Kundu, S. Mondal, S. Mukherjee, and A. Mukhopadhyay, "Spatial soil organic carbon (SOC) prediction by regression kriging using remote sensing data," *The Egyptian Journal of Remote Sensing and Space Science*, vol. 20, no. 1, pp. 61–70, 2017.
- [7] J. L. Qin, X. H. Yang, H. Fu, and X. F. Lei, "A novel nonlinear algorithm for area-wide near surface air temperature retrieval," *IEEE Journal of Selected Topics in Applied Earth Observations & Remote Sensing*, vol. 9, no. 7, pp. 3283–3296, 2016.
- [8] S. K. Kusuma, U. B. Pinnamaneni, and P. K. Kollipara, "Assessment and mapping of urban heat island using field data in the new capital region of Andhra Pradesh, India," *Journal of Science & Technology*, vol. 10, no. 11, pp. 1–8, 2017.
- [9] D. M. Amatya, A. Muwamba, S. S. Panda, T. J. Callahan, S. Harder, and C. A. Pellett, "Assessment of spatial and temporal variation of potential evapotranspiration estimated by four methods for South Carolina," *Journal of South Carolina Water Resources*, vol. 5, no. 5, pp. 3–24, 2018.
- [10] Y. Zheng, Y. He, and X. Chen, "Spatiotemporal pattern of precipitation concentration and its possible causes in the Pearl River basin, China," *Journal of Cleaner Production*, vol. 161, pp. 1020–1031, 2017.
- [11] A. Fithria and Syam'ani, "2|Fithria and Syam'ani Frequency and intensity of forest and land fire incidents in the Banjar district in 2015," *Journal of Biodiversity and Environmental Sciences*, vol. 11, no. 5, pp. 12–19, 2017.
- [12] S. Pan, S. Tian, X. Wang, L. Dai, C. Gao, and J. Tong, "Comparing different spatial interpolation methods to predict the distribution of fishes: a case study of *Coilia nasus* in the Changjiang River Estuary," *Acta Oceanologica Sinica-English Edition*, vol. 40, no. 8, pp. 119–132, 2021.
- [13] M. Moghadasi, A. N. Kalateh, and M. Rezaie, "Estimation of regularization parameter by active constraint balancing for 2D inversion of gravity data," *Journal of the Earth and Space Physics*, vol. 44, no. 3, pp. 557–573, 2018.
- [14] F. C. Wu, C. K. Wang, and G. H. Huang, "Delineation of gravel-bed clusters via factorial kriging," *Geomorphology*, vol. 308, pp. 161–174, 2018.
- [15] C. Chen, Y. Li, N. Zhao, and C. Yan, "Robust interpolation of DEMs from LiDAR-derived elevation data," *IEEE Transactions on Geoscience and Remote Sensing*, vol. 56, no. 2, pp. 1059–1068, 2017.
- [16] B. Ajvazi and K. Czimmer, "A comparative analysis of different DEM interpolation methods in GIS: case study of Rahovec, Kosovo," *Geodesy and Cartography*, vol. 45, no. 5, pp. 43–48, 2019.
- [17] Y. Yue, M. Luo, and B. Zhang, "Study on spatial distribution of DEM interpolation errors in the gully of dry-hot valley," *Wuhan Daxue Xuebao (Xinxi Kexue Ban)/Geomatics and Information Science of Wuhan University*, vol. 43, no. 7, pp. 1122–1128, 2018.
- [18] E. Alcaras, "Comparison of different interpolation methods for DEM production," *International Journal of Advanced Trends in Computer Science and Engineering*, vol. 6, no. 4, pp. 1654–1659, 2019.
- [19] M. Salah, "SRTM DEM correction over dense urban areas using inverse probability weighted interpolation and sentinel-2 multispectral imagery," *Arabian Journal of Geosciences*, vol. 14, no. 9, pp. 1–16, 2021.
- [20] R. McNabb, C. Nuth, A. Kääh, and L. Girod, "Sensitivity of glacier volume change estimation to DEM void interpolation," *The Cryosphere*, vol. 13, no. 3, pp. 895–910, 2019.
- [21] S. Khaidem, "Detection and removal of impulse noise from colour image using Lagrange interpolation and centre weighted vector median filter," *Journal of Advanced Research in Dynamical and Control Systems*, vol. 12, no. 3, pp. 50–56, 2020.
- [22] J. Wang, X. Meng, and W. Zheng, "Elastic-wave-mode separation in TTI media with inverse-distance weighted interpolation involving position shading," *Journal of Geophysics and Engineering*, vol. 14, no. 5, pp. 1260–1267, 2017.
- [23] H. Chen, L. Fang, D. L. Fan, W. Huang, and L. Zeng, "Particle swarm optimization algorithm with mutation operator for particle filter noise reduction in mechanical fault diagnosis," *International Journal of Pattern Recognition and Artificial Intelligence*, vol. 34, no. 10, p. 2058012, 2020.
- [24] H. Chen, Y. Lu, and L. Tu, "Fault identification of gearbox degradation with optimized wavelet neural network," *Shock and Vibration*, vol. 20, no. 2, p. 262, 2013.
- [25] Z. Lv, "Touch-less interactive augmented reality game on vision-based wearable device," *Personal and Ubiquitous Computing*, vol. 19, no. 3-4, pp. 551–567, 2015.
- [26] Z. Wan, Y. Dong, Z. Yu, H. Lv, and Z. Lv, "Semi-supervised support vector machine for digital twins based brain image fusion," *Frontiers in Neuroscience*, vol. 15, article 705323, 2021.
- [27] S. Wang, X. Li, K. Du, and S. Wang, "Experimental investigation of hard rock fragmentation using a conical pick on true triaxial test apparatus," *Tunnelling and Underground Space Technology*, vol. 79, pp. 210–223, 2018.
- [28] H. Wang, S. Gu, D. Wu et al., "Method for windage yaw flash-over warning of transmission lines based on numerical weather prediction," *Power System Protection & Control*, vol. 45, no. 12, pp. 121–127, 2017.
- [29] W. Tian, Z. Zhao, J. Wang, Z. Tao, and D. Yunkai, "GB-InSAR interferogram processing method to generate DEM based on

- PS technology,” *Journal of Engineering*, vol. 2019, no. 20, p. 6628, 2019.
- [30] P. M. Buscema, G. Massini, M. Fabrizi, M. Breda, and F. Della Torre, “The ANNS approach to DEM reconstruction,” *Computational Intelligence*, vol. 34, no. 1, pp. 310–344, 2018.
- [31] M. Habib, Y. Alzubi, A. Malkawi, and M. Awwad, “Impact of interpolation techniques on the accuracy of large-scale digital elevation model,” *Open Geosciences*, vol. 12, no. 1, pp. 190–202, 2020.
- [32] C. M. M. de Oliveira, M. R. Francelino, B. A. F. de Mendonça, and I. Q. Ramos, “Obtaining morphometric variables from gullies using two methods of interpolation laser scanner data: the case study of Vassouras, Brazil,” *Journal of Mountain Science*, vol. 17, no. 12, pp. 3012–3023, 2020.

RETRACTED